Aromaticity

Mono- and Multidecker Sandwich-Like Complexes of the Tetraazacyclobutadiene Aromatic Ring

Jose M. Mercero, Jon M. Matxain, and Jesus M. Ugalde*

Dedicated to Professor Cecilia Sarasola

Since the fortuitous discovery[1] of ferrocene, $[(C_5H_5)_2Fe]$, the cyclopentadienyl anion has emerged as the most versatile aromatic ring for the synthesis of sandwich-like complexes. Indeed, it has been estimated that more than 80% of all known organometallic complexes of transition metals contain a substituted or unsubstituted cyclopentadienyl ligand.[2] Nevertheless, new aromatic compounds have recently been identified whose incorporation into sandwich complexes opens new routes for chemical creativity. In particular, we have predicted[3] that the all-metal $[Al_4]^{2-}$ aromatic ring[4] can complex Ti to form $[Al_4TiAl_4]^{2-}$.

The tetraazacyclobutadiene dianion, N_4^{2-}, also fulfills the aromaticity requirements.[5] It has a square-planar structure with six delocalized π electrons, four of which occupy the nonbonding π highest occupied molecular orbitals (HOMOs); the other two π electrons participate effectively in the aromatic stabilization, in agreement with the $(4n+2)$ rule. The nucleus-independent chemical shift (NICS)[6] at 1.0 Å above the molecular plane is −4.09 ppm,[7] confirming further the π-aromatic character of the ring. Consequently, N_4^{2-} can, in principle, be incorporated into sandwich-like complexes although, as far as we know, no such structures have been reported to date.

We have therefore theoretically characterized stable sandwich-type complexes of the N_4^{2-} aromatic ring with early (Ti, V, and Cr) and late (Fe, Co, and Ni) transition-metal centers, with charges 2− (Ti, Fe), 1−(V, Co), and 0 (Cr, Ni). The optimized structure of the Ti sandwich-like complex has D_{4h} symmetry; the V and Cr analogues have C_{2v} symmetry, although they can also be viewed as bent D_{4h} structures (Figure 1). The optimum geometries of the late-transition-metal complexes have D_{4d} symmetry. Consequently, for the complexes of the early-transition metals the nitrogen atoms are eclipsed whereas they are staggered for those of the late transition metals.

The calculations were carried out with the B3LYP functional, as implemented in Gaussian 98,[8] with the standard 6-311G basis set.

[*] J. M. Mercero, J. M. Matxain, J. M. Ugalde
Kimika Fakultatea
Euskal Herriko Unibertsitatea
P.K. 1072; 20080 Donostia, Euskadi (Spain)
Fax: (+34) 94-3015-270
E-mail: pobmelat@sq.ehu.es

Supporting information for this article is available on the WWW under http://www.angewandte.org or from the author.

 DOI: 10.1002/ange.200460498

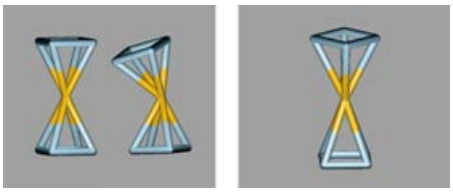

Figure 1. The eclipsed D_{4h} and C_{2v} structures of the early transition metals (right) and the staggered D_{4d} structure of the late transition metals (left; blue N, orange metal center).

The geometrical properties, charges at the metal, and the NICS of the N_4 squares of both the early- and late-transition-metal complexes are collected in Table 1. The increase in the N–N bond length is appreciably larger upon complexation of N_4^{2-} with the early transition metals than with the late ones. Concomitantly the square–metal distances (Sq–TM in Table 1) are longer for the early-transition-metal complexes, which is indicative of the subtle N_4^{2-} ring–metal interactions in these complexes.

Table 1: Properties of the molecules (calculated at the B3LYP/6-311G level of theory) described in the text.[a]

	Transition metal						
	Ti	V	Cr	Fe	Co	Ni	N_4^{2-}
Symm.	D_{4h}	C_{2v}	C_{2v}	D_{4d}	D_{4d}	D_{4d}	D_{4h}
Charge	−2	−1	0	−2	−1	0	−2
Sq-TM	1.850	1.780	1.740	1.694	1.678	1.692	–
N–N	1.492	1.49	1.49	1.476	1.458	1.456	1.445
Sq-TM-Sq	180.0	152.6	140.4	180.0	180.0	180.0	
CHELP	1.350	1.485	0.999	0.566	0.524	0.466	
NICS(0)	39.0	64.9	73.6	−5.78	−5.45	4.00	9.2
NICS(1)	10.9	17.3	19.3	−16.80	−11.14	−3.00	−4.19
EDE_{ad}	−2.66	3.74	–	−2.49	6.586	−8.74[b]	
EDE_{ovgf}							
HOMO	−3.97	5.04	10.47	–	4.992	11.09	
p.s.	0.86	0.90	0.91	–	0.90	0.87	
HOMO-1	–	5.05		–	4.992	11.09	
p.s.	–	0.90		–	0.90	0.87	
HOMO-2	–	5.72		−0.39	5.788		
p.s.	–	0.91		0.90	0.91		
HOMO-3	–	5.46			5.788		
p.s.	–	0.92			0.91		

[a] Charges refer to the net charge of the complex. The bond lengths (Where Sq-TM stands for the distance between the center of the square and the metal) are given in Å. Atomic charges in e^- are calculated using the CHELP[9] method. EDE_{ad} are in eV and EDE_{ovgf} also in eV with their associated pole strengths (p.s.) and the orbital from which the electron is detached. NICS are given in ppm. [b] The resulting cation corresponds to the rearranged $Ni(N_2)_4^+$ complex, rather than to a sandwich-like complex.

The main difference between the early- and late-transition-metal complexes, however, is found in the aromaticity of the N_4 ring upon complexation. Despite its widespread use, aromaticity is more of a theoretical concept than a directly measurable quantity. Consequently, measurements of aromaticity are based on many different criteria.[10] Among them, the NICS, which is based on the "absolute magnetic shielding" at the center of a ring compound, is widely used and has proven to be accurate for ordinary cyclic carbon compounds. This method has also recently been successfully applied to inorganic cyclic aromatic compounds.[11,12] Nevertheless, it is worth mentioning that relying on a single aromaticity indicator probably gives an incomplete picture. However, analysis of the NICS values of the tetraazacyclobutadiene moiety nicely shows how early- and late-transition-metal centers behave differently towards complexation with N_4^{2-}.

Thus, the NICS value of N_4^{2-} at the center of the molecular plane, NICS(0), is 9.2 ppm and the value at 1.0 Å above the molecular plane, NICS(1), is −4.19 ppm; that is, N_4^{2-} is σ antiaromatic and π aromatic. Complexation with the early-transition-metal centers enhances the σ antiaromaticity of the N_4^{2-} ring and destroys its π aromaticity, as revealed by the very positive values of both NICS(0) and NICS(1). It should be noted, however, that the geometry of the tetraazacyclobutadiene moiety in the early-transition-metal complexes is still a square, despite the antiaromaticity predicted by the NICS values. On the other hand, for the later-transition-metal centers, and in particular for Fe and Co, the remarkable enhancement of both the σ and the π aromaticity renders the N_4 ring doubly aromatic, a concept first introduced by Schleyer and co-workers[13] and then experimentally confirmed by Berndt and co-workers.[14,15] Nickel does not alter the σ antiaromatic and π aromatic character of the N_4^{2-} ring upon complexation.

In Figure 2 we show the HOMO−2 a_1 orbital of the $[N_4FeN_4]^{2-}$ complex, which has σ delocalization of the N_4 rings. This orbital might be responsible for the remarkable enhancement of the σ aromaticity of the iron complex relative to the analogous Ti complex. The orbital that correlates with the a_1 orbital of the iron complex is the a_{1g} orbital in the Ti complex, which is unoccupied, as shown in Figure 2. Accordingly, π antiaromaticity has to be expected for the N_4 rings of the iron complex, since the occupied e_2 doubly degenerate HOMO orbitals are of π-antibonding character with respect to the N_4 rings, as shown in Figure 2.

The NICS(1) values, however, tell another story. While all the early-transition-metal complexes are π antiaromatic, the late ones are π aromatic. This is presumably because the occupation of the two degenerate e_2 orbitals triggers the π-aromaticity contribution of the internal orbitals of

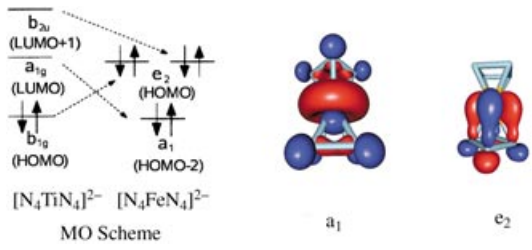

Figure 2. The MO scheme shows the correspondence between the $[N_4TiN_4]^{2-}$ (D_{4h}) and $[N_4FeN_4]^{2-}$ (D_{4d}) valence orbitals. The orbitals shown are the a_1 (left) and the doubly degenerate e_2 (right) orbitals of the $[N_4FeN_4]^{2-}$ (D_{4d}) complex.

the complex (see the Supporting Information). Schleyer and co-workers have demonstrated recently that the aromaticity is determined by the contribution of *all* the π/σ-orbitals of the system.[11] CMO-NICS calculations[16] (CMO = canonical molecular orbitals) will help to confirm this point further.

We have also focused our attention on the stability of the mono- and dianionic complexes, as they can lose an electron due to the intramolecular coulombic repulsion, and dissociate. The dianionic complexes (Ti and Fe), indeed, have negative electron-detachment energies (EDE), thus indicating that the monoanions are more stable than the dianions. However, the complexes with charge −1 (V and Co) have positive EDEs, which confirms their stability towards electron detachment. We therefore calculated both the adiabatic[17] electron-detachment energies, EDE_{ad}, and the unrestricted outer valence Green's functions electron-detachment energies, EDE_{ovgf}.[18] All give qualitatively the same picture, as shown in Table 1.

EDEs are one key property for the experimental characterization of these complexes, as shown recently by Li et al.[4] in their photoelectron spectroscopy investigation of $[Al_4]^{2-}$ stabilized against Coulomb explosion by an alkali-metal cation. We have followed their approach for the dianionic sandwich-like complexes of Ti and Fe, and have characterized their structures in the presence of one Li^+ and two Li^+ ions. We found that the cation(s) can interact with the complex at various positions although, for the sake of brevity, the properties of only the most stable structures (see Figure 3) are given in Table 2.

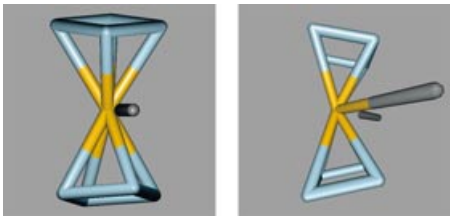

Figure 3. Most stable structures of $[LiN_4XN_4]^-$ (left) and $[Li_2N_4XN_4]$ (right, X = Ti,Fe; blue N, orange X, gray Li).

Once the cation(s) interact(s) with the complex, the EDE become positive and the resulting complex becomes stable towards electron detachment. This stability increases significantly upon interaction with the second lithium atom. Consequently, these complexes might be suitable for experimental manipulation. The aromatic properties of the N_4 rings remain similar upon interaction with the cation(s). Thus, the N_4 rings of the Ti complex remain σ and π antiaromatic, while the rings of the iron complex retain their σ and π aromaticity; the enormous enhancement of the σ aromaticity of the N_4 rings of $[LiN_4FeN_4]^-$ should be noted.

As has been mentioned above the dianionic complexes of Ti and Fe are unstable with respect to electron loss due to Coulomb repulsion and, therefore, probably have very short lifetimes. The stabilization of dianions for their experimental manipulation is normally carried out by forming their lithium salts, like those of the $[Al_4]^{2-}$ inorganic aromatic dianion[4] and

Table 2: Properties of the $[N_4XN_4]^{2-}\cdot Li_n^+$ complexes ($n = 1,2$; X = Ti,Fe). (see the description in Table 1).

	Ti		Fe	
	Li	2 Li	Li	2 Li
Symmetry	C_{2v}	C_s	C_{2v}	C_{2v}
Charge	−1	0	−1	0
N–N	1.49/1.46	1.45/1.49	1.48/1.45	1.43/1.47
Sq–TM	1.856	1.87/1.83	1.697	1.712
TM–Li	2.711	2.89/2.63	2.273	2.407
N–Li	1.903	1.94/2.01	1.983	2.029
sq-TM-sq	146.9	137.8	172.4	167.70
Li-TM-Li	–	79.91	–	101.6
TM (CHELP)	1.19	1.31	0.99	0.30
Li (CHELP)	0.70	0.54/0.58	0.52	0.80
BE	257.67	395.61	247.5	391.77
NICS(0)	27.64	26.26	−116.9	−22.3
NICS(1)	8.70	8.92	−31.9	−6.89
EDE_{ad}	1.78	6.11	1.13	7.43
EDE_{ovgf}				
HOMO	0.45	5.03	4.70	8.78
p.s.	0.868	0.871	0.908	0.915
HOMO-1	4.12	9.03	4.50	9.391
p.s.	0.892	0.896	0.916	0.906
HOMO-2	4.70	9.11	5.43	10.589
p.s.	0.892	0.886	0.915	0.907

$C_2H_2^{2-}$ organic aromatic dianion.[19] The interaction of the $[N_4XN_4]^{2-}$ dianions with Li^+ ions yields a remarkable energetic stabilization. The lithium stripping energies [Eq. (1)],

$$[Li_nN_4XN_4]^{n-2} \rightarrow [N_4XN_4]^{2-} + n\,Li^+;\ n = 1;\ X = Ti,\ Fe \qquad (1)$$

are 257.8 and 247.5 kcal mol^{-1} for the Ti and Fe monolithium complexes, respectively, and 395.6 and 391.8 kcal mol^{-1} for the respective dilithium complexes, which suggests that these species might be stable enough to be handled experimentally. Additional evidence for the stability of the dianions comes from an inspection of the energy of the following reaction [Eq. (2)]:

$$[Li_2N_4XN_4]^{n-2} \rightarrow 2N_4^{2-} + 2Li^+ + X^{2+};\ X = Ti \qquad (2)$$

which is 1223.7 kcal mol^{-1} for X = Ti and 1302.0 kcal mol^{-1} for X = Fe. The corresponding reaction energy for ferrocene [Eq. (3)]:

$$[(C_5H_5)_2Fe] \rightarrow 2(C_5H_5)^{-1} + Fe^{2+} \qquad (3)$$

is 656.0 kcal mol^{-1},[20,21] and the energy of the reaction in Equation (4):

$$[Li_2N_4] \rightarrow 2Li^+ + N_4^{2-} \qquad (4)$$

is 455.1 kcal mol^{-1}.[7]

Multidecker structures or even polymers of transition metal–aromatic ring complexes are common.[22] However, early and late transition metals induce different structural patterns. Thus, Kaya and Nakajima have shown recently that Sc, Ti, and V form multidecker structures,[23] while Fe, Co, and Ni form "rice-ball" structures where all the metal atoms are

clustered at the center and surrounded by the aromatic molecules.

Our calculations demonstrate that both early and late transition metals can form highly linear, multidecker complexes of formula $[TM_n(N_4)_{n+1}]^{2-}$. Titanium, in particular, forms linear, multidecker complexes where the first two N_4 units of both ends are eclipsed with the remaining units being staggered. Conversely, for iron the disposition of all adjacent N_4 units is staggered.

Figure 4 shows the optimum structures of $[Ti_7(N_4)_6]^{2-}$ and $[Fe_7(N_4)_8]^{2-}$, which are molecular complexes of about 2.4 nm in length. The vibrational harmonic frequencies of all the so-far characterized oligomers can be found in the Supporting Information, as they might be useful for their experimental detection.

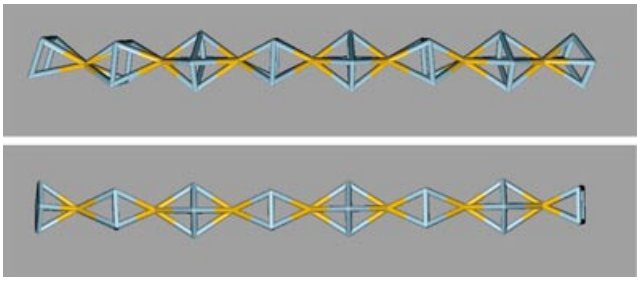

Figure 4. Optimum structures of $[Ti_7(N_4)_8]^{2-}$ (top) and $[Fe_7(N_4)_8]^{2-}$ (bottom) multidecker structures (blue N, orange metal center).

The HOMO–LUMO energy gaps of these multidecker complexes of Ti and Fe are collected in Table 3.

Table 3: The HOMO–LUMO energy gap (eV) for multidecker $[TM_n(N_4)_{n+1}]^{2-}$ complexes (TM = Ti, Fe).

n	Ti	Fe
3	1.245	2.846
4	1.150	2.275
5	0.932	1.798
6	0.754	1.472
7	0.600	1.343

The trend shown in Table 3 is that the HOMO–LUMO gap decreases with an increase in the number of monomer units in the structure. Consequently, since the band gap is controlled by the size of the oligomeric structure, these materials could be useful as semiconductors in nanostructure devices. It should also be possible to synthesize one-dimensional polymeric wires of these materials. Such wires would have a very narrow band gap and would hence behave as conducting one-dimensional polymers.

In summary, we have reported on the possibility of incorporating the aromatic N_4^{2-} dianion into transition-metal sandwich-like complexes. Interestingly, these sandwich-like complexes may also form multidecker structures and eventually condense into one-dimensional polymers. The structures predicted here await experimental verification.

Received: April 29, 2004

Keywords: aromaticity · density functional calculations · sandwich complexes · transition metals

[1] T. J. Kealy, P. L. Pauson, *Nature* **1951**, *168*, 1039.
[2] C. Janiak, H. Schumann, *Adv. Organomet. Chem.* **1991**, *33*, 291.
[3] J. M. Mercero, J. M. Ugalde, *J. Am. Chem. Soc.* **2004**, *126*, 3380.
[4] X. Li, A. E. Kuznetsov, H. F. Zhang, A. I. Boldyrev, L.-S. Wang, *Science* **2001**, *291*, 859.
[5] G. Van Zandwijk, R. A. J. Janssen, H. M. Buck, *J. Am. Chem. Soc.* **1990**, *112*, 4155.
[6] A negative NICS value signifies an electron current at the point where it is calculated; it signals the aromatic character of the molecule.
[7] Q. S. Li, L. P. Cheng, *J. Phys. Chem. A* **2003**, *107*, 2882.
[8] Gaussian 98 (Revision A.11), M. J. Frisch, G. W. Trucks, H. B. Schlegel, G. E. Scuseria, M. A. Robb, J. R. Cheeseman, V. G. Zakrzewski, J. A. Montgomery, R. E. Stratmann, J. C. Burant, S. Dapprich, J. M. Millam, A. D. Daniels, K. N. Kudin, M. C. Strain, O. Farkas, J. Tomasi, V. Barone, M. Cossi, R. Cammi, B. Mennucci, C. Pomelli, C. Adamo, S. Cli ord, J. Ochterski, G. A. Petersson, P. Y. Ayala, Q. Cui, K. Morokuma, D. K. Malick, A. D. Rabuck, K. Raghavachari, J. B. Foresman, J. Cioslowski, J. V. Ortiz, B. B. Stefanov, G. Liu, A. Liashenko, P. Piskorz, I. Komaromi, R. Gomperts, R. L. Martin, D. J. Fox, T. Keith, M. A. Al-Laham, C. Y. Peng, A. Nanayakkara, C. Gonzalez, M. Challacombe, P. M. W. Gill, B. G. Johnson, W. Chen, M. W. Wong, J. L. Andres, M. Head-Gordon, E. S. Replogle, J. A. Pople, Gaussian, Inc., Pittsburgh, PA, **2001**.
[9] L. E. Chirlian, M. M. Francl, *J. Comput. Chem.* **1987**, *8*, 894.
[10] V. I. Minkin, M. N. Glukhovtsev, B. Y. Simkin, *Aromaticity and Antiaromaticity*, Wiley, New York, USA, **1994**.
[11] Z. Cheng, C. Corminboeuf, T. Heine, J. Bohmann, P. v. R. Schleyer, *J. Am. Chem. Soc.* **2003**, *125*, 13930.
[12] Y. Jung, T. Heine, P. v. R. Schleyer, M. Head-Gordon, *J. Am. Chem. Soc.* **2004**, *126*, 3132.
[13] J. Chandrasekhar, E. D. Jemmis, P. v. R. Schleyer, *Tetrahedron Lett.* **1979**, *20*, 3707.
[14] M. Unverzagt, G. Subramanian, M. Hofmann, P. v. R. Schleyer, S. Berger, K. Harms, W. Massa, A. Berndt, *Angew. Chem.* **1997**, *109*, 1469; *Angew. Chem. Int. Ed. Engl.* **1997**, *36*, 1469.
[15] C. Präsang, A. Mlodzianowska, Y. Sahin, M. Hofmann, G. Geiseler, W. Massa, A. Berndt, *Angew. Chem.* **2002**, *114*, 3380; *Angew. Chem. Int. Ed.* **2002**, *41*, 3380.
[16] T. Heine, C. Corminboeuf, P. v. R. Schleyer, G. Seifert, R. Reviakine, J. Weber, *J. Phys. Chem. A* **2003**, *107*, 6470.
[17] The adiabatic EDE is taken to be the difference between the energies of the dianion and the monoanion at their optimal geometries.
[18] W. v. Niessen, J. Schirmer, L. S. Cederbaum, *Comput. Phys. Rep.* **1984**, 157.
[19] A. Sekiguchi, T. Matsuo, M. Tanaka, *Organometallics* **2002**, *21*, 1072.
[20] M. F. Ryan, J. R. Eyler, D. E. Richardson, *J. Am. Chem. Soc.* **1992**, *114*, 8611.
[21] A. Irigoras, J. M. Mercero, I. Silanes, J. M. Ugalde, *J. Am. Chem. Soc.* **2001**, *123*, 5040.
[22] T. J. Peckham, P. Gómez-Elipe, I. Manners, *Metallocenes*, *Vol. 2* (Eds.: A. Togni, R. L. Halterman), Wiley-VCH, Weinheim, **1998**, p. 724.
[23] A. Nakajima, K. Kaya, *J. Phys. Chem. A* **2000**, *104*, 176.

